Electronic Supplementary Material (ESI) for ChemComm.

This journal is © The Royal Society of Chemistry 2024

Supporting Information

Ligand-engineering Cu-based catalysts to accelerate the electrochemical reduction of CO_2

Ying Liang,[a] Rui Zhang,[b] Kaihong Xiao,[a] Fenghui Ye,[a] Xinyue Ma,[a] Wei Liu,*[c] Hanle Yin,[a] Baoguang Mao,*[a] Xiangru Song,[a] Chuangang Hu*[a]

a. State Key Laboratory of Organic-Inorganic Composites, College of Chemical Engineering, Beijing University of Chemical Technology, Beijing 100029, China

b. Engineering and Technology Research Center of Membranes for Chemical Industry, Beijing University of Chemical Technology, Beijing 100029, China

c. College of Materials Science and Engineering, Beijing University of Chemical Technology, Beijing 100029, P. R. China

Experimental details

Materials

Copper nitrate trihydrate [$Cu(NO_3)_2$] and p-Phenylenediamine ($C_6H_8N_2$) were purchased from Macklin (Shanghai), China. Piperazine hexahydrate ($C_4H_{10}N_2 \cdot 6H_2O$) and absolute ethanol (C_2H_5OH) were purchased from Sigma-Aldrich (Merck KGaA), Germany. Commercial Cu powder, commercial copper phthalocyanine (CuPc), and commercial Cu_2O were all purchased from Aladdin (Shanghai), China. Nafion D-520 dispersion (5 wt% in lower aliphatic alcohol and water) was purchased from Suzhou Sinero Technology Co., Ltd. CeTech carbon cloth (W1S1011) was purchased from Beijing Nano-Catalyst Technology Co., Ltd. Nafion 211 proton exchange membrane was purchased from Shanghai Hesen Electric Co., Ltd. Ultrapure water at 18.25 MΩ·cm was prepared by a Classics ELGA purification system (Anhui Laboury Instrument & Technology, China). All reagents and chemicals were obtained commercially and used without further purification.

Synthesis of Cu-PR and Cu-pPDA

The Cu-PR (copper-piperazine) catalyst was prepared through a direct stirring method. Specifically, 1942 mg of piperazine hexahydrate and 234 mg of $Cu(NO_3)_2$ were dissolved in 50 mL of deionized water separately and ultrasonicated for 30 min to obtain a uniform solution. Then, the piperazine solution was dropwise added to the $Cu(NO_3)_2$ solution. The above solution was stirred in an ice bath at 800 r/min for 5 hours, the resulting light blue suspension was centrifuged and washed three times with ethanol and deionized water. Subsequently, the obtained solid was frozen with liquid nitrogen and followed by lyophilization, to obtain the Cu-PR catalyst. The synthesis process of Cu-pPDA (copper-p-Phenylenediamine) is similar to that of Cu-PR, except that the mass of the reactants was changed. Specifically, 1081 mg of p-Phenylenediamine and 234 mg of $Cu(NO_3)_2$ were weighed and used as reactants.

Preparation of cathode electrodes

The catalyst ink was prepared by dissolving 1 mg of catalyst powder in the mixture of 790 μL ethanol and 200 μL deionized water followed by the addition of 10 μL of Nafion

solution. The resulting mixture was ultrasonicated for 15 min to uniformly disperse. Then, the resulting slurry was drop-coated on WIS-1011 carbon cloth to achieve a catalyst loading of 1 mg cm^{-2}. The electrode was then dried in the atmosphere for the subsequent electrochemical testing experiments.

Characterizations

The band gap of the material was determined by UV-visible absorption spectroscopy (Varian Cary 6000i) in the wavelength range 190-800 nm. Fourier transform of infrared (FTIR) was equipped with a DLaTGS detector to measure the infrared spectrum (FT-IR) of a sample. For infrared spectroscopy, the sample is prepared by taking a certain amount of powdered sample and an appropriate amount of solid potassium bromide, which is then fully ground and pressed to test the sample. Scanning electron microscopy (SEM) images were obtained using a JSM6700-F working at 10 kV. Transmission electron microscope (TEM) images were recorded by a FEIT 20 working at 200 kV. X-ray diffraction (XRD) patterns were acquired on a Bruker D8 Advance diffractometer with a Cu Kα source equipped with a Lynxeye one-dimensional detector. The X-ray photoelectron spectrometer (XPS) was an ECSALAB 250Xi instrument from the U.S.A. Sample preparation required rubbing the powdered sample onto conductive tape and then wrapping and pressing it with aluminum foil. X-ray adsorption spectroscopy (XAS) measurements of the powder samples were measured in transmission mode at the 1W1B station in Beijing Synchrotron Radiation Facility (BSRF).

Electrochemical measurements

The electrochemical test was performed with a CHI760E electrochemical station, using a gas-tight H-cell which was separated into a two-compartment cell by Nafion 211 membrane. The H-cell contained a cathode compartment and an anode compartment, the cathode compartment contained catalyst electrodes and Ag/AgCl as the working and reference electrode, respectively, whereas the anode compartment used platinum sheets as a counter electrode. 0.1 M $KHCO_3$ electrolyte was utilized as the electrolyte for the CO_2 reaction. Before conducting CO_2 electro-reduction, CO_2 gas was introduced into the electrolyte and ventilated for more than 30 minutes to reach a saturated CO_2 solution (pH = 6.8). The average flow rate of CO_2 gas was 30 $mL \cdot min^{-1}$ with continuous

stirring at a rate of 500 rpm during the electrocatalysis process. Linear sweep voltammetry (LSV) was conducted at a scan rate of 5 mV s^{-1} with the potential corrected for iR (90%) loss. After the LSV was stabilized and overlapped, a fixed voltage was applied to sweep the current time curves (i-t), and after 10 minutes, the gas phase composition was analyzed by gas chromatography (GC). All potentials used in this study were converted into the reversible hydrogen electrode (RHE), and the reference using the following equation: E (*vs.* RHE) = E (*vs.* Ag/AgCl) + 0.197 V + 0.0591 × pH.

Gaseous and liquid products analysis

The gaseous product in the electrochemical experiment was analyzed by GC (HP 4890D). The liquid products were quantified using a nuclear magnetic resonance spectrometer (^{1}H NMR). The ^{1}H NMR spectra were collected on the Bruker Avance III HD 400 spectrometer. In order to accurately quantify the product, dimethyl sulfoxide (DMSO) was used as a standard reagent in the ^{1}H NMR analysis. Each sample consists of 500 μL electrolyte, 100 μL D_2O and 100 μL 10mM DMSO solution.

The calculation of turnover frequency (TOF, h^{-1}):

the TOF for a certain product was calculated by the equation:

$$TOF = \frac{I_{product}/NF}{\omega m_{cat}/M_{Cu}} \times 3600$$

$I_{product}$: partial current for certain product;

N: the number of electrons transferred for product formation, which is 2 for CO;

F: Faradaic constant, 96485 C mol^{-1};

m_{cat}: catalyst mass in the electrode, g;

ω: Cu loading in the catalyst;

M_{Cu}: atomic mass of Cu, 63.55 g mol^{-1}.

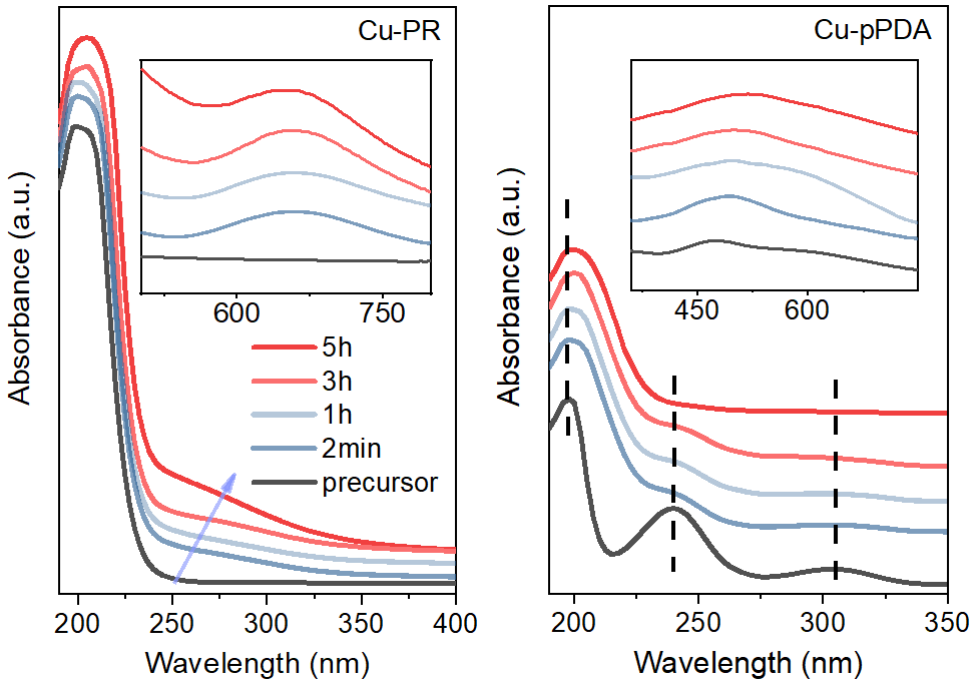

Fig. S1. UV-vis absorption spectroscopy of reaction solutions at different stages during the synthesis of Cu-PR and Cu-pPDA.

The UV-Vis spectra were employed to monitor the structure evolution of the typical samples at different reaction times. Firstly, the PR monomer shows the characteristic peak at ~200nm, while the characteristic peaks of pPDA are 197nm, 240nm, and 305nm. When Cu^{2+} ions were mixed with the PR and pPDA monomers, respectively, Cu (II)-complexes were immediately formed. As the reaction time increased, their complexes underwent ligand-to-metal charge transfer induced by the electron donation (from the coordinated PR/pPDA to Cu element). Consequently, this led to the gradual oxidative polymerization of PR and pPDA, and simultaneously partial reduction of Cu (II) to produce Cu-PR and Cu-pPDA, respectively.

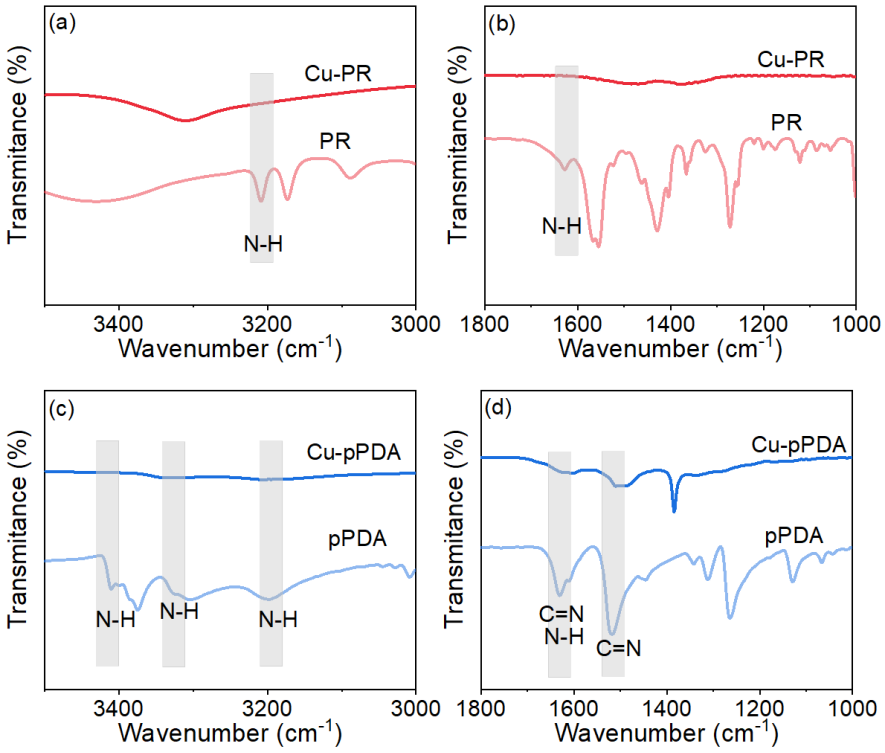

Fig. S2. Partial enlarged images of FT-IR for Cu-PR and Cu-pPDA.

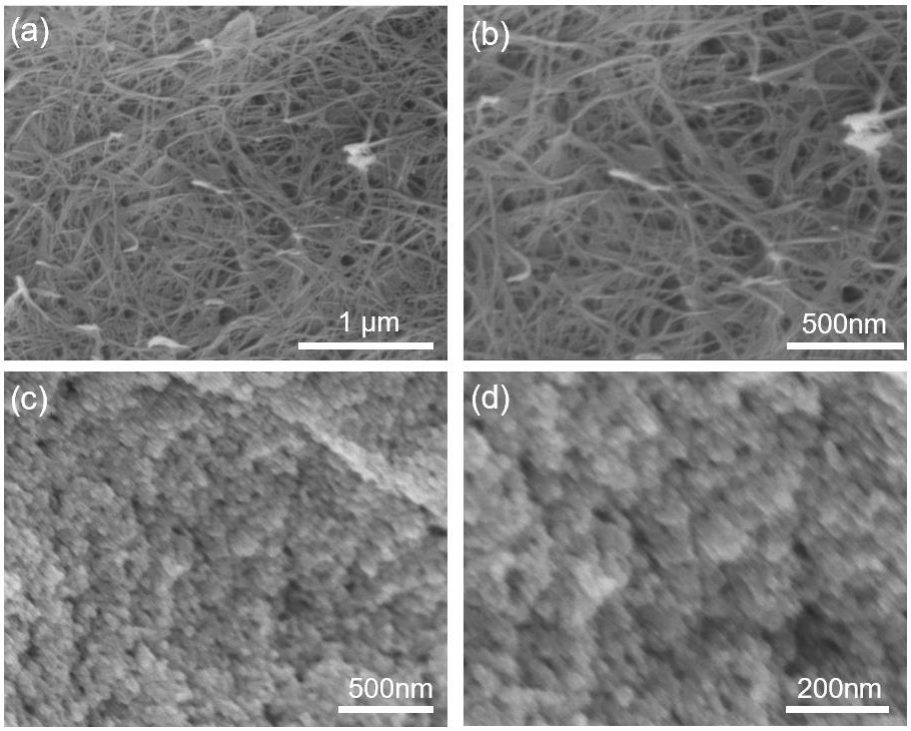

Fig. S3. SEM images of (a,b) Cu-PR and (c,d) Cu-pPDA.

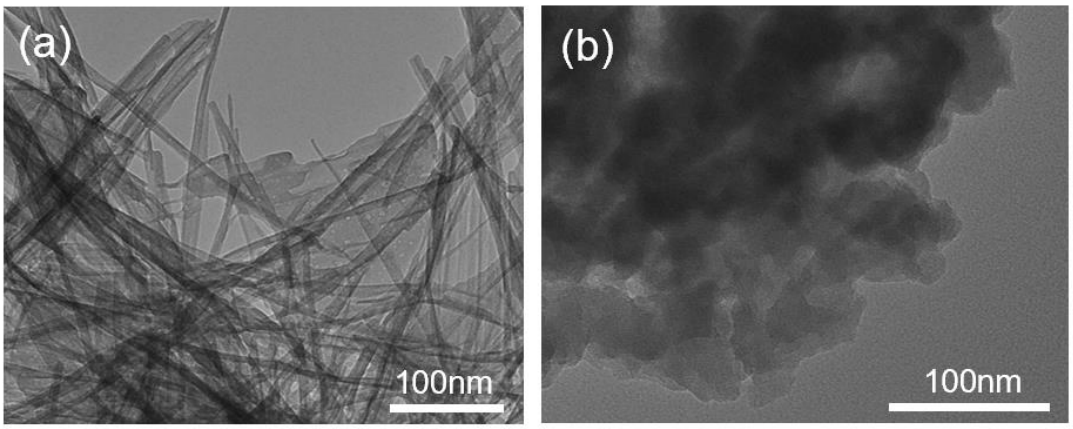

Fig. S4. TEM images of (a) Cu-PR and (b) Cu-pPDA.

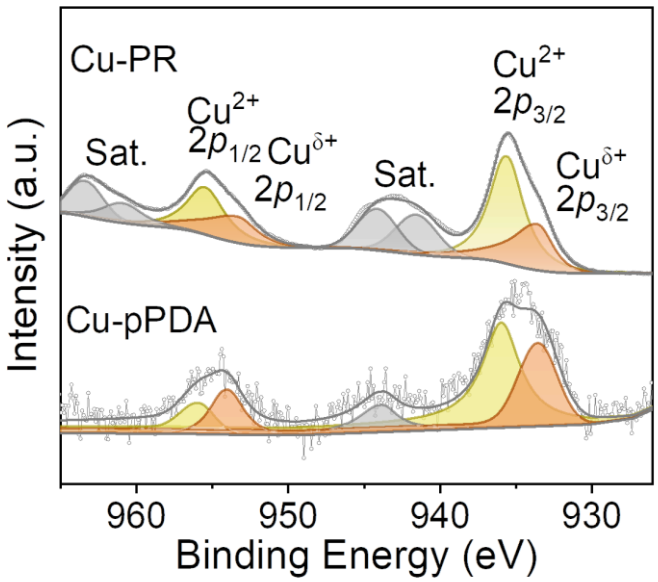

Fig. S5. Cu 2p XPS spectra of Cu-PR and Cu-pPDA.

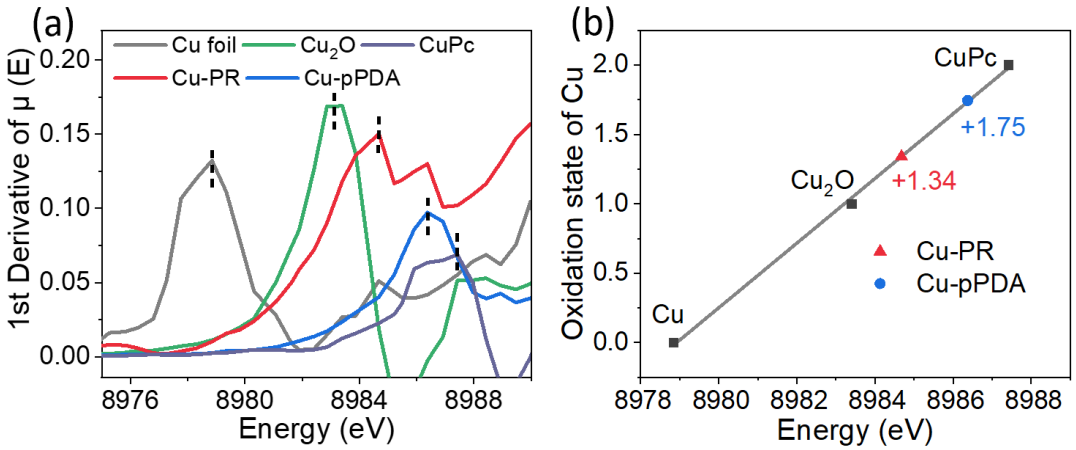

Fig. S6. (a) Cu K-edge of first derivative spectra, (b) linear fitting curve of Cu valence state.

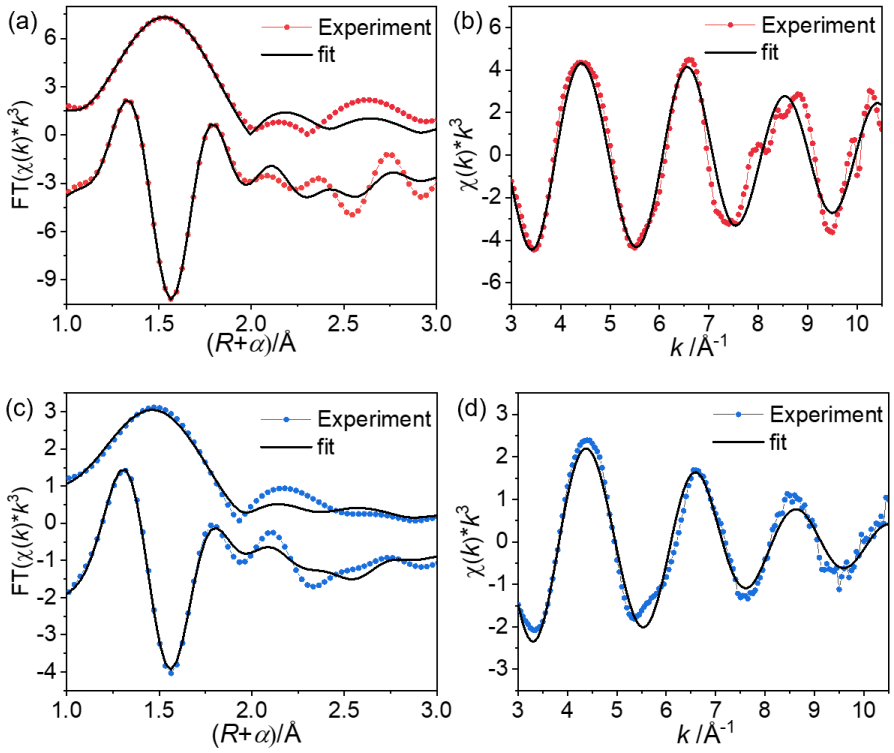

Fig. S7. Cu K-edge EXAFS (points) and fitting curves (line) for Cu-PR shown in (a) R-space and (b) k^3-weighted k-space, and Cu-pPDA shown in (c) R-space and (d) k^3-weighted k-space. The data is not phase-corrected.

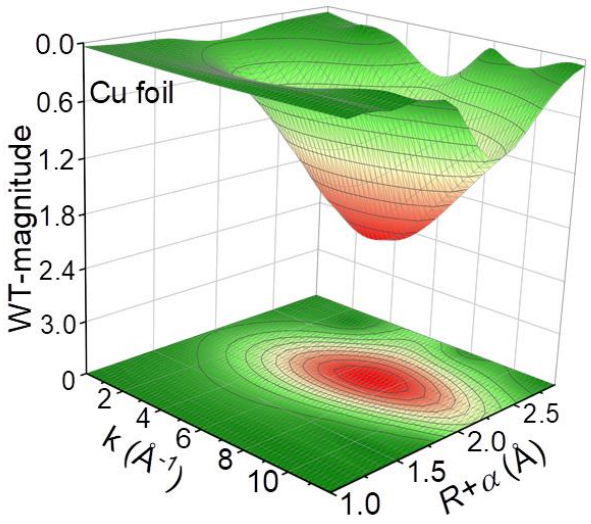

Fig. S8. WT k^3-weighted EXAFS contour plot of Cu foil.

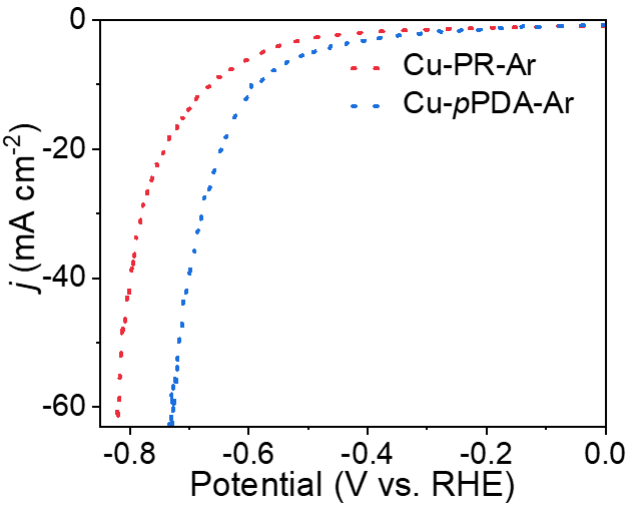

Fig. S9. LSV curves for Cu-PR-Ar and Cu-pPDA-Ar in 0.1 M Ar-saturated $KHCO_3$ electrolyte.

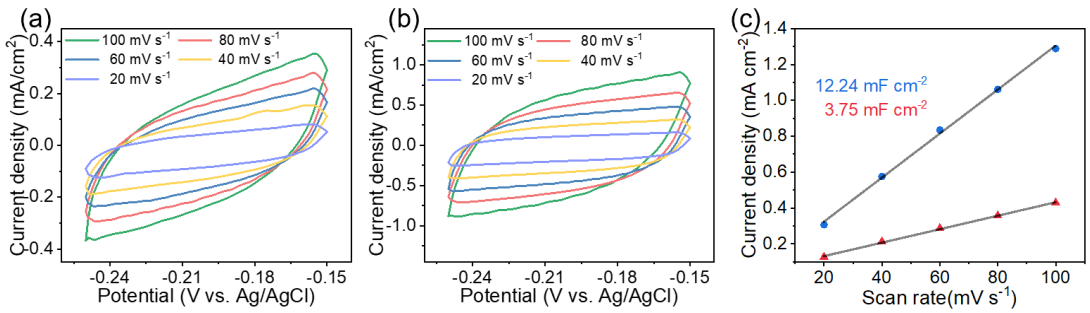

Fig. S10. Typical cyclic voltammograms at scan rates ranging from 20 to 100 mV s^{-1} or (a) Cu-PR and (b) Cu-pPDA. (c) Corresponding relationship of current density and scan rates. The blue mark represents Cu-pPDA, and the red represents Cu-PR.

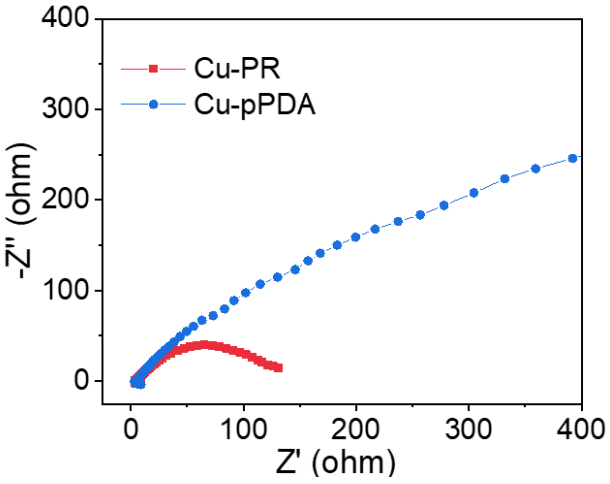

Fig. S11. Nyquist plots of Cu-PR and Cu-pPDA.

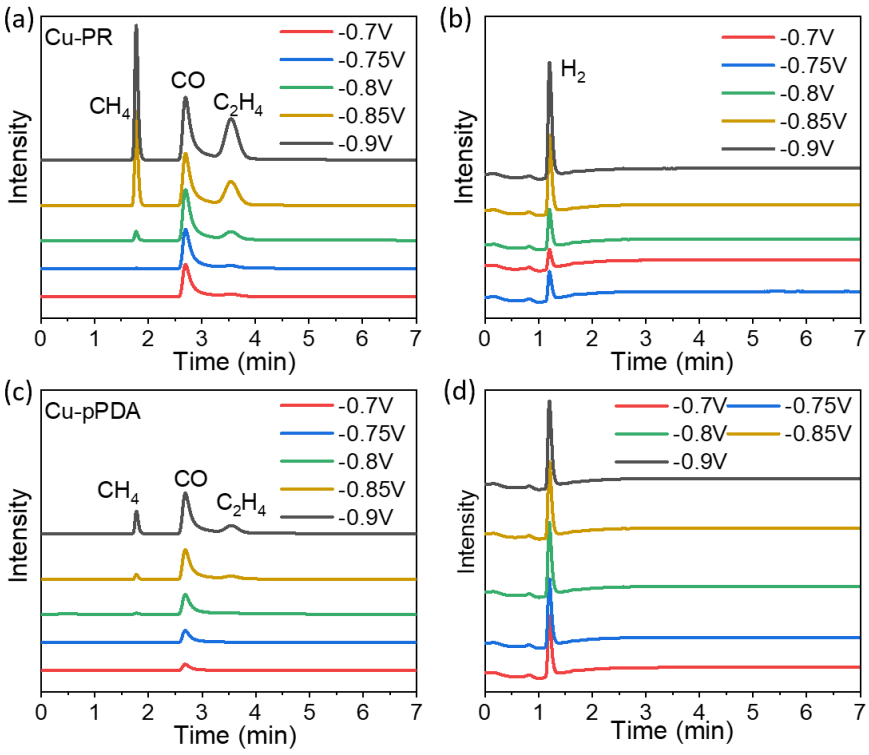

Fig. S12. GC data of (a,b) Cu-PR and (c,d) Cu-pPDA at different potentials.

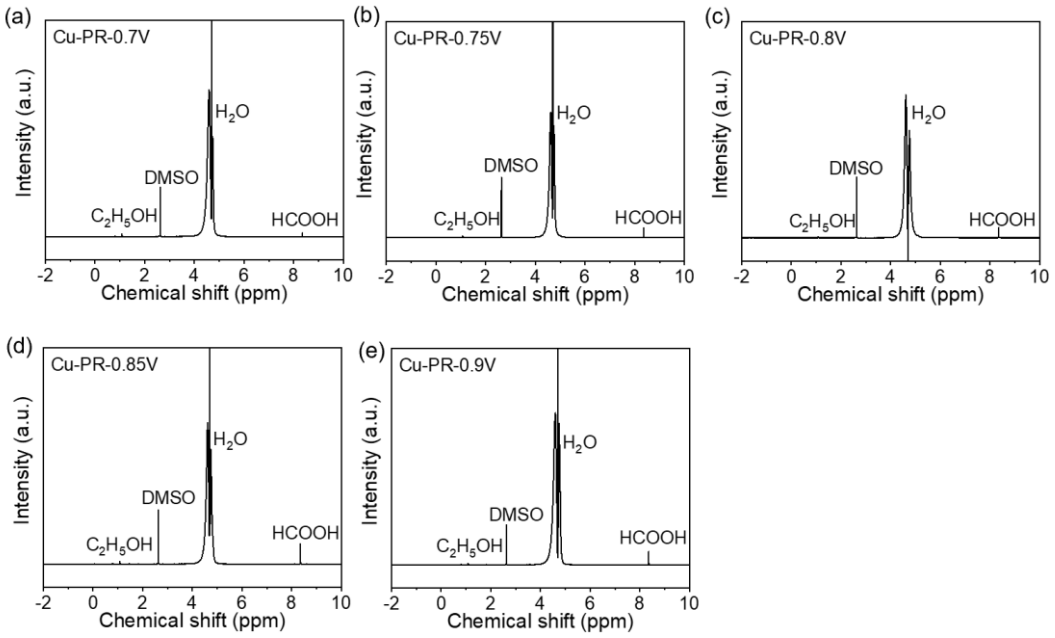

Fig. S13. ^{1}H NMR for the liquid products of Cu-PR at different potentials.

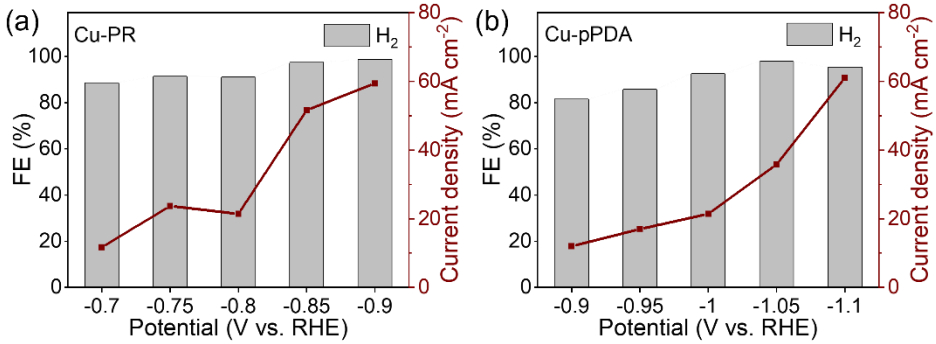

Fig. S14. FEs of (a) Cu-PR and (b) Cu-pPDA in Ar-saturated 0.1 M $KHCO_3$ electrolyte, respectively.

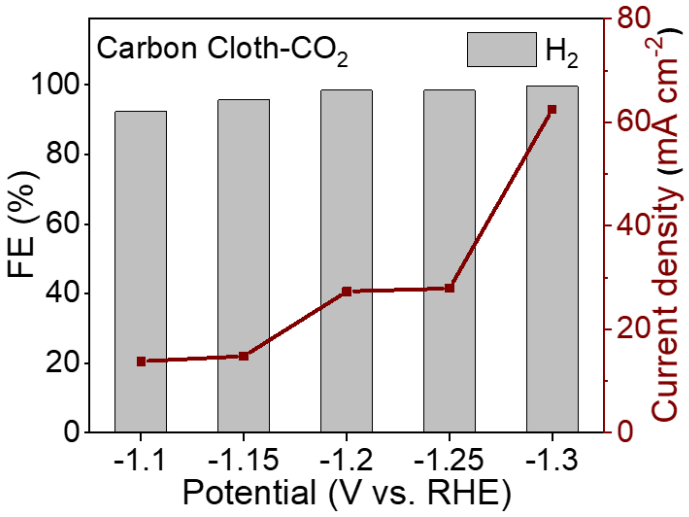

Fig. S15. FE of carbon cloth in CO_2-saturated 0.1 M $KHCO_3$ electrolyte.

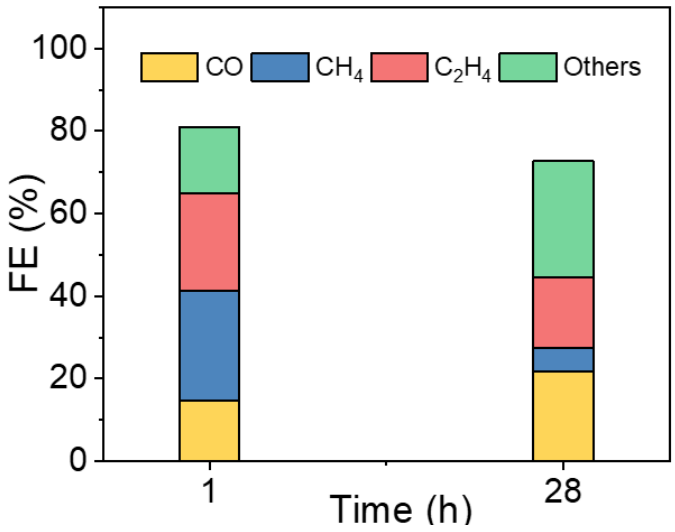

Fig. S16. FE distribution of Cu-PR at the potential of -0.8 V *vs.* RHE.

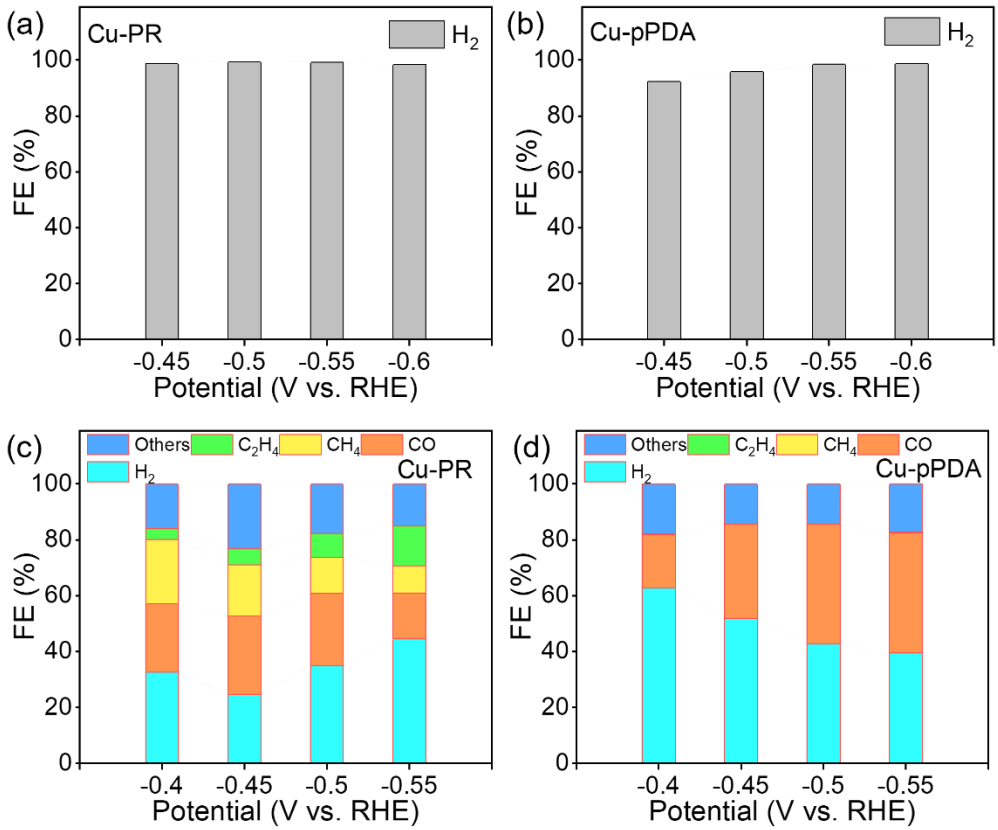

Fig. S17. (a,b) FEs of Cu-PR and Cu-pPDA in CO_2-saturated 0.05 M H_2SO_4 electrolyte. (c,d) FEs of Cu-PR and Cu-pPDA in CO_2-saturated 0.1 M KOH electrolyte.

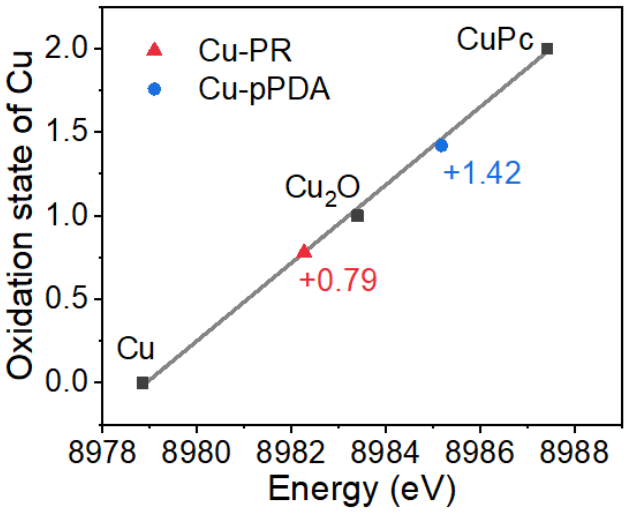

Fig. S18. Linear fitting curve of Cu valence state.

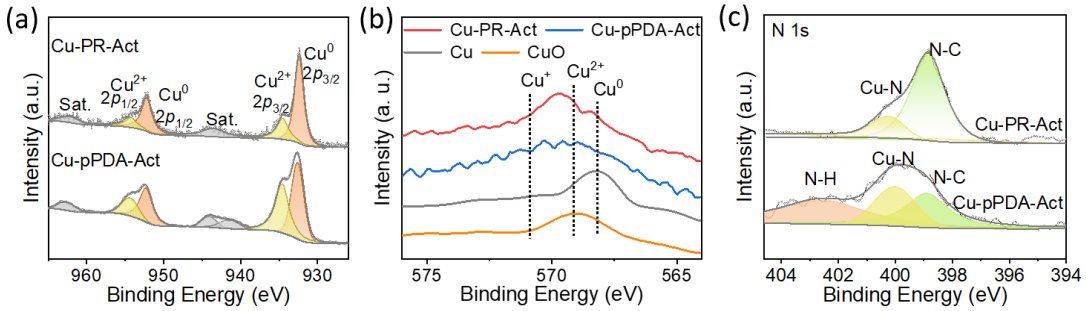

Fig. S19. (a) Cu 2p XPS spectra of Cu-PR-Act and Cu-pPDA-Act. (b) Cu LMM spectra of Cu-PR-Act, Cu-pPDA-Act, and standard samples. (c) N 1s XPS spectra of Cu-PR-Act and Cu-pPDA-Act.

The intensity of Cu^{2+} peaks in Cu-PR-Act is significantly reduced, while Cu-pPDA-Act is basically unchanged. The Cu LMM spectrum for Cu-PR-Act shows a pronounced peak attributed to Cu^0 compared to the initial Cu-PR, proving that metallic Cu was formed after electrochemical activation. In addition, Cu-N peaks can still be observed in the N 1s XPS spectra of Cu-PR-Act and Cu-pPDA-Act, but the intensity of the Cu-N peak is significantly lower in Cu-PR-Act.

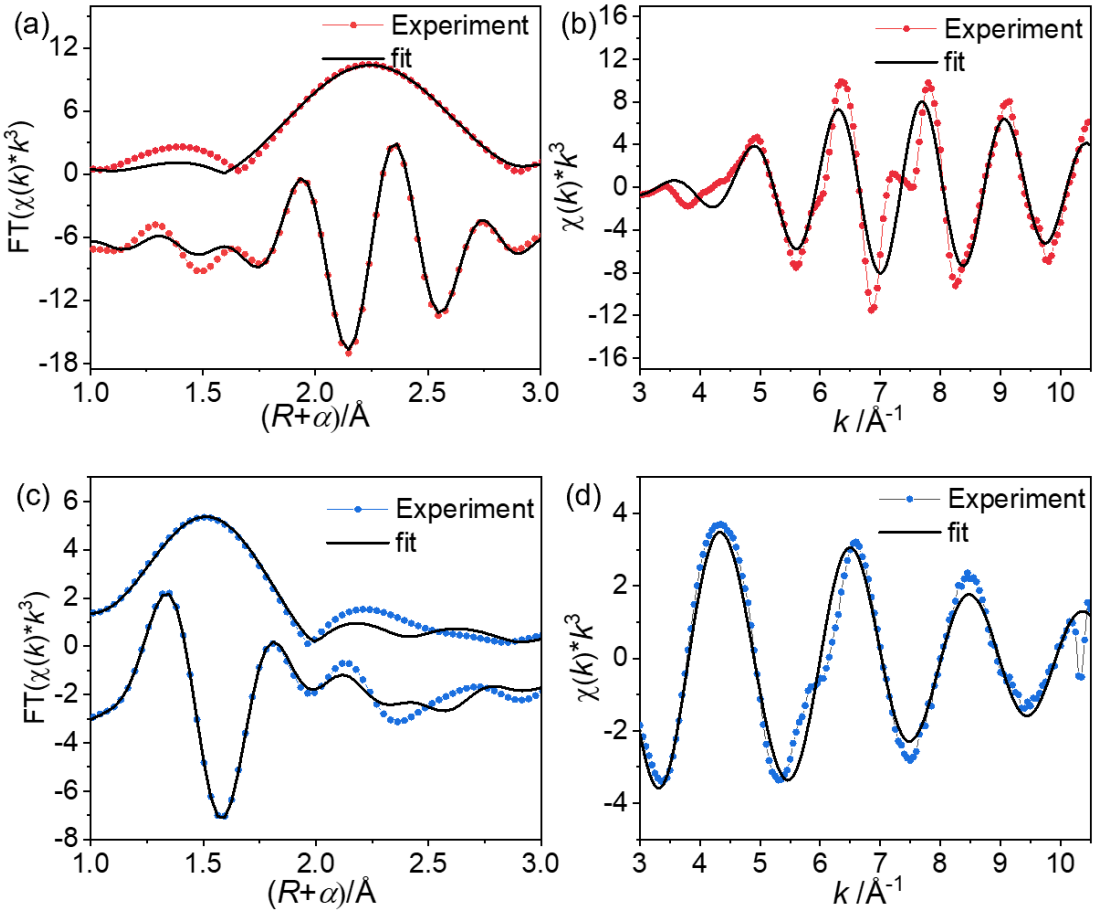

Fig. S20. Cu K-edge EXAFS (points) and fitting curves (line) for Cu-PR-Act of (a) R-space and (b) k^3-weighted k-space. Cu K-edge EXAFS (points) and fitting curves (line) for Cu-pPDA-Act of (c) R-space and (d) k^3-weighted k-space. The data is not phase-corrected.

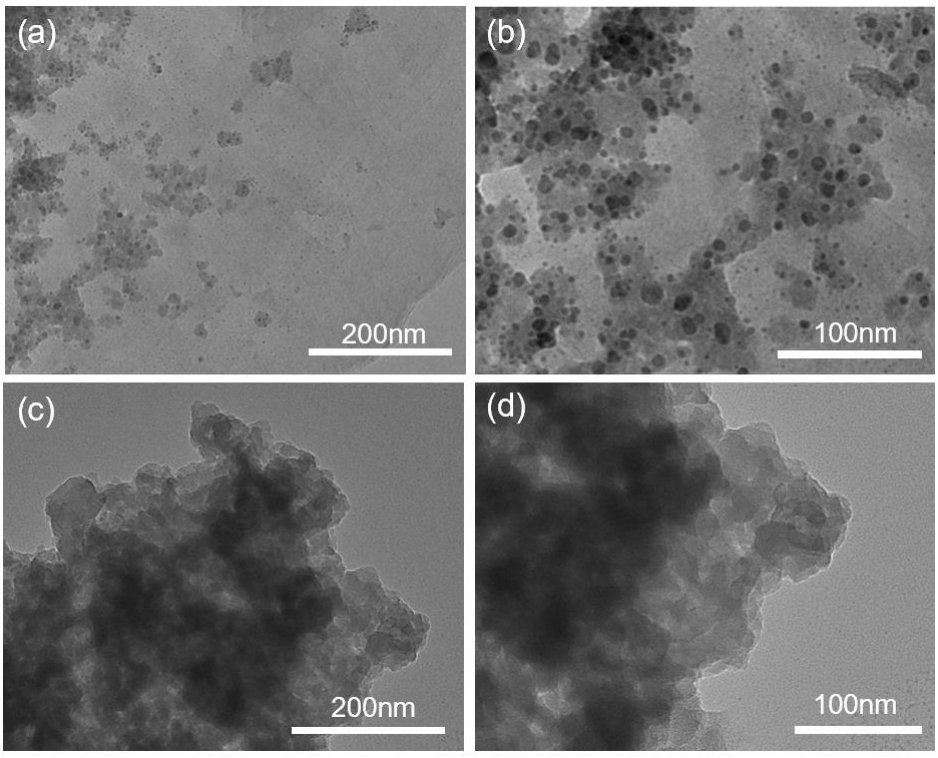

Fig. S21. TEM images of (a,b) Cu-PR, and (c,d) Cu-pPDA after *in situ* electrochemical activation.

Table S1. The fitting structural parameters of Cu K-edge EXAFS data for Cu-PR and Cu-pPDA.

Catalysts	Path	CN	R(Å)	σ^2 (Å^2)	ΔE_0 (eV)	R-factor
Cu-PR	Cu–N	4.2±0.6	1.96±0.01	0.004	8.259	0.016
Cu-pPDA	Cu–N	3.3±0.3	1.94±0.01	0.008	2.970	0.018

CN is the coordination number; R is the interatomic distance (bond length from center atom to coordination atom); σ^2 represents the Debye-Waller factor in evaluating thermal and static disorder in absorber-scatterer distances; ΔE_0 indicates edge-energy shift; R factor is used to value the accuracy of the fitting; S_0^2 indicates the amplitude reduction factor and is fixed as 0.839 (obtained by the fitting of Cu foil). The selected k-ranges for EXAFS fitting are 3-10.5. The R-range is between 1 Å to 3 Å.

Table S2. The fitting structural parameters of Cu K-edge EXAFS data for Cu-PR-Act and Cu-pPDA-Act.

Catalysts	Path	CN	R(Å)	σ^2 (Å^2)	ΔE_0 (eV)	R-factor
Cu-PR-Act	Cu–Cu	7.2±1.7	2.55±0.01	0.009	5.710	0.011
Cu-pPDA-Act	Cu–N	3.0±0.4	1.96±0.01	0.006	5.124	0.017